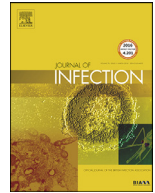




Since January 2020 Elsevier has created a COVID-19 resource centre with free information in English and Mandarin on the novel coronavirus COVID-19. The COVID-19 resource centre is hosted on Elsevier Connect, the company's public news and information website.

Elsevier hereby grants permission to make all its COVID-19-related research that is available on the COVID-19 resource centre - including this research content - immediately available in PubMed Central and other publicly funded repositories, such as the WHO COVID database with rights for unrestricted research re-use and analyses in any form or by any means with acknowledgement of the original source. These permissions are granted for free by Elsevier for as long as the COVID-19 resource centre remains active.



Letter to the Editor

The lung tissue microbiota features of 20 deceased patients with COVID-19



To the Editor

We read with great interest the article by Yanan Chu and colleagues, accepted for publication in the Journal of Infection.¹ Secondary infection and sepsis are common complications in critically ill patients with COVID-19,^{2,3} but the underlying pathogen is not clear. We investigated the microbiota characteristics of lung tissue from 20 deceased COVID-19 patients. All cases met the COVID-19 clinical diagnostic criteria provided by the National Health Commission of China, and died at Union Hospital, Tongji Medical College, Huazhong University of Science and Technology, Wuhan, between February 1, 2020, and March 31, 2020. The median age was 66 years (interquartile range, IQR, 60.75–77.0 years), 16 (80%) were older than 60 years and 14 (70.0%) were male. One patient had a history of exposure to the Huanan seafood market. On admission, most patients had fever (15 [75.0%]) and cough (15 [75.0%]). Half of the patients had dyspnoea (10 [50.0%]) and fatigue or myalgia (10 [50.0%]). One-fifth of the patients had diarrhoea (4 [20%]). Other symptoms included chest pain, vomiting and headache. All 20 (100.0%) patients had findings of bilateral infiltrates on radiographic imaging. Fifteen (75.0%) patients had comorbidities, including cardiovascular disease (10 [50%]), hypertension (9 [45%]), malignancy (7 [35.0%]), diabetes (2 [10.0%]), chronic kidney disease (2 [10.0%]), and chronic lung disease (1 [5%]). The median time from symptom onset to hospital admission was 10 days (IQR, 6.75–14 days). The median time from hospital admission to death was 23 days (IQR, 20–30 days). Measures of vital signs were recorded on the day of hospital admission for all patients. The patients often developed tachypnoea, and the median respiratory rate was 25 (IQR, 20–30 breaths per minute). The patients had a median percutaneous oxygen saturation of 92% (IQR, 86.8%–97.3%) on admission. The most common complications were respiratory failure (20 [100%]) and sepsis (18 [90%]), followed by liver dysfunction (17 [85%]), acute respiratory distress syndrome (14 [70%]), acute kidney injury (14 [70%]) and acute cardiac injury (14 [60%]). All patients received antibacterial therapy (20 [100%]) and antiviral therapy (20 [100%]). Most patients received glucocorticoid therapy (18 [90%]), and 12 patients received antifungal therapy (60%). In terms of ventilation modes, 4 patients (20%) received noninvasive ventilation, and invasive mechanical ventilation was required in 16 patients (80%). A total of 5 patients (25%) received continuous kidney replacement therapy (Table 1). In agreement with previous studies, our study confirmed that older men (>65 years) and those with comorbidities (especially malignancy) were more vulnerable to SARS-CoV-2 infection. Notably, sepsis was the most frequently observed complication. Immediately after death, post-mortem needle core biopsies were performed on bilateral lungs in

the negative-pressure isolation ward. The procedures were guided with ultrasound, and specimens were collected aseptically. Tissue cores were fixed in 10% neutral formalin immediately after being removed from the body, fixed for over 24 h, dehydrated in a graded series of ethanol, cleared in xylene, and then embedded in paraffin. A QIAamp DNA Mini Kit (QIAGEN, Hilden, Germany) was used to extract the total DNA from every FFPE tissue. The V3-V4 regions of the 16S rRNA samples were amplified by PCR, and the specific primers were 338F: 5-*ACTCCTACGGGAGGCAGCA*-3 and 806R: 5-*GGACTACHVGGGT WTCTAAT*-3. The ITS1 genes were amplified using barcoded ITS 5F: 5-*GGAAGTAAAAGTCGTAACAAGG*-3 and ITS1R: 5-*GCTGCGTTCTTCATCGATGC*-3. The quantified amplicons were pooled in equal amounts, and pair-end 2 × 300 bp sequencing was performed using the Illumina MiSeq platform with a MiSeq Reagent Kit v3. The sequencing data were analysed using QIIME V1.8.0 package. The bacterial distribution was characterized by the relative abundance of operational taxonomy units (OTUs). The most prevalent genera were *Acinetobacter* (80.70% of the total sequences), *Chryseobacterium* (2.68%), *Burkholderia* (2.00%), *Brevundimonas* (1.18%), *Sphingobium* (0.93%), and *Enterobacteriaceae* (0.68%), together comprising 92.32% of the total sequences and regularly detected in all subjects. *Mycobacterium* (3.59%) and *Prevotella* (0.56%) were detected mainly in patients 19 and 20 (Fig. 1A). The fungal community in the lung microbiome of each patient was analysed by ITS gene sequencing. The most common genus was *Cutaneotrichosporon* (*Cryptococcus*, 28.14%), followed by *Issatchenkia* (8.22%), *Wallemia* (4.77%), *Cladosporium* (4.67%), *Alternaria* (4.46%), *Dipodascus* (4.01%), *Mortierella* (3.22%), *Aspergillus* (2.72%), *Naganishia* (2.53%), *Diatina* (2.15%), and *Candida* (1.42%). Each patient's fungal infection status is shown in a heat map (Fig. 1B). More remarkably, the vast majority of patients had mixed bacterial and fungal infections.

Although originally believed to be sterile, the lung exhibits a microbiota that varies in both physiological and pathological conditions.⁴ Many authors agree that healthy lung tissue has a low density of microbial populations, represented mainly by genera such as *Prevotella*, *Veillonella*, *Streptococcus* and *Tropheryma*.⁵ In our study, disorder of the lung microbiome was characterized by enrichment with the OTU of the *Acinetobacter* spp., which is usually comprised of *Acinetobacter calcoaceticus*, *Acinetobacter baumannii*, *Acinetobacter nosocomialis*, and *Acinetobacter pittii*, with *Acinetobacter baumannii* (AB) being the most clinically important species responsible for the highest incidence of multidrug resistance and mortality.⁶ It should be noted that Enterobacteriaceae spp., a kind of abundant taxonomic group in the human gut microbiome, was common in the lung tissues of fatal COVID-19 patients. The *Enterobacteriaceae* family of bacteria (a kind of taxon comprising many potentially pathogenic bacteria including *Klebsiella*, *Escherichia coli*, *Proteus*, *Enterobacter*, etc.) might release a large amount of endotoxin in the intestinal lumen, which would

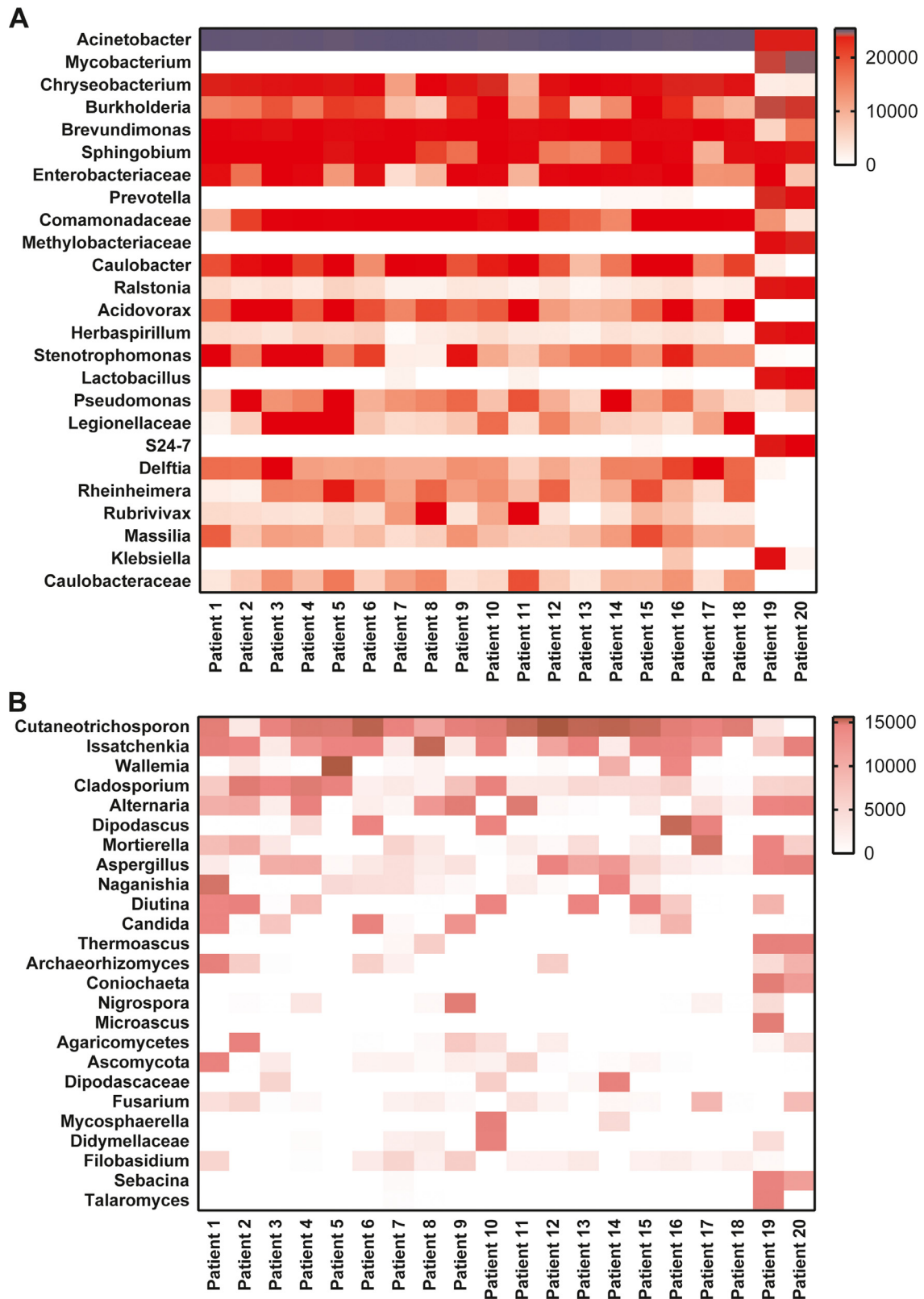


Fig. 1. (A) Distribution of bacterial genera (OTUs) found in the lung samples of fatal COVID-19 patients defined by sequencing of the 16S rRNA gene. (B) Distribution of fungal genera (OTUs) found in the lung samples of fatal COVID-19 patients defined by sequencing of the ITS gene. Increasing depth of colour indicates the relative abundance of the OTU in an individual sample.

Table 1
Demographic Characteristics of fatal Patients With COVID-19.

Characteristics	n = 20, n (%)
Median (IQR) age, years	66 (60.75–77)
<40 years	1 (5)
40–60 years	3 (15)
≥60 years	16 (80)
Sex	
Female	6 (30)
Male	14 (70)
Huanan Seafood Market exposure	1 (5)
Initial common symptoms	
Fever	15 (75)
Cough	15 (75)
dyspnea	10 (50)
Chest pain	1 (5)
Headache	1 (5)
Vomiting	1 (5)
Diarrhoea	4 (20)
Fatigue or myalgia	10 (50)
Chest imaging, infiltrate	
Unilateral	0 (0)
Bilateral	20 (100)
Comorbidities	
Hypertension	9 (45)
Diabetes	2 (10)
Cardiovascular disease	10 (50)
Chronic lung diseases	1 (5)
Chronic kidney disease	2 (10)
Malignancy	7 (35)
Median (IQR) time from onset of symptom to hospital admission, days	10 (6.75–14)
Median (IQR) time from hospital admission to death, days	23 (20–30)
Vital signs on admission	
Disorders of consciousness	0 (0)
Median (IQR) arterial pressure, mm Hg	137 (120–150)
Median (IQR) heart rate, beat per minute	91 (79–103)
Median (IQR) respiratory rate, breaths per minute	25 (20–30)
Median (IQR) percutaneous oxygen saturation,	92% (86.8%–97.3%)
Complications	
Sepsis	18 (90)
Respiratory failure	20 (100)
Acute respiratory distress syndrome	14 (70)
Liver dysfunction	17 (85)
Acute kidney injury	14 (70)
Acute cardiac injury	12 (60)
Treatment	
Antibacterial therapy	20 (100)
Antiviral therapy	20 (100)
Antifungal therapy	12 (60)
Glucocorticoids therapy	18 (90)
Intravenous immunoglobulin therapy	11 (55)
Interferon inhalation	3 (15)
Oxygen treatment	
High flow nasal cannula	1 (5)
Noninvasive ventilation	3 (15)
Invasive mechanical ventilation	16 (80)
Continuous renal replacement therapy	5 (25)
Extracorporeal membrane oxygenation	0 (0)

inhibit protein synthesis in intestinal epithelial cells.⁷ Significantly, we observed that the fungal communities in lung specimens were usually dominated by *Cryptococcus* spp. *Cryptococcus* infections have high morbidity and mortality rates worldwide, particularly in the context of immune suppression and central nervous system involvement.⁸ Moreover, we successfully detected *Issatchenkia* spp., *Cladosporium* spp., *Cladosporium* spp., *Alternaria* spp., *Aspergillus* spp., and *Candida* spp., all of which are important species for opportunistic invasive mycosis in immunocompromised patients. In general, persistent lymphocytic depletion, mechanical ventilation, corticosteroid therapy and prolonged hospital stays may lead to the development of opportunistic infections in fatal COVID-19. What is more important is that fatal COVID-19 is associated with complex mixed bacteria and fungal infections in the lungs. Therefore, it is urgent to serially monitor the microbiota in the lower respiratory tract for timely personalized treatment.

Declaration of Competing Interest

All authors declare no competing interests.

Ethics approval

The study was approved by the health commission of Hubei Province and the ethics committee of Union Hospital, Tongji Medical College, Huazhong University of Science and Technology (approval number: 2020-0043-1).

Acknowledgments

We thank all patients and their families involved in the study. This study was financially supported by grant from the Key Special Project of [Ministry of Science and Technology](#), China

(No.2020YFC 0845700); the National Natural Science Foundation of China (No. 81773022); the Fundamental Research Funds for the Central Universities (No. 2020 kfyXG YJ101).

References

1. Chu Y, Li T, Fang Q, Wang X. Clinical features of critically ill patients with confirmed COVID-19. *J. Infect.* Jul 2020;**81**(1):147–78 PubMed PMID: 32360498.
2. Zhou F, Yu T, Du R, Fan G, Liu Y, Liu Z, et al. Clinical course and risk factors for mortality of adult inpatients with COVID-19 in Wuhan. *China: Retrospect Cohort Study. Lancet* 2020 Mar 11 PubMed PMID: 32171076.
3. Chen T, Wu D, Chen H, Yan W, Yang D, Chen G, et al. Clinical characteristics of 113 deceased patients with coronavirus disease 2019: retrospective study. *Bmj* 2020 Mar 26;**368**:m1091 PubMed PMID: 32217556.
4. Beck JM, Young VB, Huffnagle GB. The microbiome of the lung. *Transl Res: J Lab Clin Med* Oct 2012;**160**(4):258–66 PubMed PMID: 22683412. Pubmed Central PMCID: 3440512.
5. Man WH, de Steenhuijsen Piters WA, Bogaert D. The microbiota of the respiratory tract: gatekeeper to respiratory health. *Nat Rev Microbiol* May 2017;**15**(5):259–70 PubMed PMID: 28316330. Pubmed Central PMCID: 7097736.
6. Doi Y, Murray GL, Peleg AY. *Acinetobacter baumannii*: evolution of antimicrobial resistance-treatment options. *Semin Respir Crit Care Med* Feb 2015;**36**(1):85–98 PubMed PMID: 25643273. Pubmed Central PMCID: 4465586.
7. Zeng Y, Chen S, Fu Y, Wu W, Chen T, Chen J, et al. Gut microbiota dysbiosis in patients with hepatitis B virus-induced chronic liver disease covering chronic hepatitis, liver cirrhosis and hepatocellular carcinoma. *J. Viral Hepat.* Feb 2020;**27**(2):143–55 PubMed PMID: 31600845.
8. Levitz SM, Dupont MP, Smail EH. Direct activity of human T lymphocytes and natural killer cells against *Cryptococcus neoformans*. *Infect. Immun.* Jan 1994;**62**(1):194–202 PubMed PMID: 8262627. Pubmed Central PMCID: 186086.

Jun Fan[#], Xiang Li[#]

Department of pathology, Union Hospital, Tongji Medical College,
Huazhong University of Science and Technology, Wuhan 430022,
China

Yong Gao[#]

Department of Orthopaedics, Union Hospital, Tongji Medical College,
Huazhong University of Science and Technology, Wuhan 430022,
China

Junjie Zhou

Department of pathology, Union Hospital, Tongji Medical College,
Huazhong University of Science and Technology, Wuhan 430022,
China

Sihua Wang

Department of Thoracic surgery, Union Hospital, Tongji Medical
College, Huazhong University of Science and Technology, Wuhan
430022, China

Bo Huang, Junhua Wu, Qin Cao, Yajun Chen, Zhenkang Wang,
Danju Luo

Department of pathology, Union Hospital, Tongji Medical College,
Huazhong University of Science and Technology, Wuhan 430022,
China

Ting Zhou, Ruiting Li, You Shang¹

Department of Critical Care Medicine, Union Hospital, Tongji Medical
College, Huazhong University of Science and Technology, Wuhan
430022, China

Xiu Nie^{*1}

Department of pathology, Union Hospital, Tongji Medical College,
Huazhong University of Science and Technology, Wuhan 430022,
China

*Corresponding author.

E-mail addresses: whunhpath@163.com, niexiuyishi@126.com (X.
Nie)

[#] J.F., X.L. and Y.G. contributed equally to this work. X.N. and
Y.S. contributed equally to this work.